Hindawi Publishing Corporation
Journal of Engineering
Volume 2014, Article ID 839128, 9 pages
http://dx.doi.org/10.1155/2014/839128

Research Article

Adaptive Vibration Control of Piezoactuated Euler-Bernoulli Beams Using Infinite-Dimensional Lyapunov Method and High-Order Sliding-Mode Differentiation

Teerawat Sangpet,[1] Suwat Kuntanapreeda,[1] and Rüdiger Schmidt[2]

[1]*Department of Mechanical and Aerospace Engineering, King Mongkut's University of Technology North Bangkok, 1518 Pracharat Sai 1, Bangkok 10800, Thailand*
[2]*Institute of General Mechanics, RWTH Aachen University, Templergraben 64, 52056 Aachen, Germany*

Correspondence should be addressed to Teerawat Sangpet; teerawat.me@gmail.com

Received 31 July 2014; Revised 26 November 2014; Accepted 8 December 2014; Published 22 December 2014

Academic Editor: Jyoti Sinha

This paper presents an adaptive control scheme to suppress vibration of flexible beams using a collocated piezoelectric actuator-sensor configuration. A governing equation of the beams is modelled by a partial differential equation based on Euler-Bernoulli theory. Thus, the beams are infinite-dimensional systems. Whereas conventional control design techniques for infinite-dimensional systems make use of approximated finite-dimensional models, the present adaptive control law is derived based on the infinite-dimensional Lyapunov method, without using any approximated finite-dimension model. Thus, the stability of the control system is guaranteed for all vibration modes. The implementation of the control law requires a derivative of the sensor output for feedback. A high-order sliding mode differentiation technique is used to estimate the derivative. The technique features robust exact differentiation with finite-time convergence. Numerical simulation and experimental results illustrate the effectiveness of the controller.

1. Introduction

Flexible structures have attracted interest because of their lighter weight compared to traditional structures. They have been widely used in aerospace applications and robotics [1–3]. However, the flexibility leads to vibration problems. Therefore, vibration control is needed. Over the past few decades, active vibration control has drawn more interests from researchers since it can effectively suppress the vibration [4–7].

Piezoelectric actuators and sensors provide an effective means of vibration suppression of flexible structures [8]. The advantages of using piezoelectric actuators and piezoelectric sensors include nanometer scale resolution, high stiffness, and fast response. Many researchers have studied the vibration suppression of flexible structures using piezoelectric actuators and piezoelectric sensors. In [9], Tavakolpour et al. proposed a self-learning vibration control strategy for flexible plate structures. A control algorithm is based on a P-type iterative learning with displacement feedback. Wang et al. [10] presented a simple control law for reducing the vibration of the flexible structure. Linear feedback control was derived using a linear matrix inequality method. Qiu et al. [11] proposed a neural network controller based on PD control with collocated piezoelectric actuator and sensor. The back-propagation algorithm was utilized for adapting the controller parameters. In [12], Sangpet et al. utilized a fractional-order control approach to improve the delay margin in the control system of a piezoactuated flexible beam. The controller parameters were tuned experimentally. An et al. [13] presented a time-delay acceleration feedback controller for vibration suppression of cantilever beams. Stability boundaries of the closed-loop system were determined by a Hurwitz stability criterion. In [14], Takács et al. presented an adaptive-predictive vibration control system using extended Kalman filter. The viability of the control method was

experimentally evaluated. In [15], Sangpet et al. proposed an observer-based hysteresis compensation scheme for tracking control of a piezoactuated flexible beam. The observer based on a PI observer and a Kalman-filter algorithm was employed for estimation of the hysteresis in the beam. The scheme was successfully implemented in experimental tests.

The governing equation of vibrating flexible structures is a partial differential equation (PDE). Thus, the systems are distributed-parameter systems and have an infinite number of vibration modes. Most of control design techniques exploit an approximated finite-dimensional model by ignoring the higher frequency modes. However, this approach can cause the control system to become unstable due to a spillover effect [16, 17].

Infinite-dimensional control for the systems modeled by PDEs has been recently investigated. Extensions of finite-dimensional techniques to infinite-dimensional systems as well as innovative infinite-dimensional specific control design approaches have been proposed; see [18] and references therein. The Lyapunov-based control method has played a major role in nonlinear control of finite-dimensional complex systems [19–22]. Infinite-dimensional Lyapunov-based control is its extension to infinite-dimensional systems, which has been successfully applied to many engineering problems [23–28].

In [23], Dadfarnia et al. proposed infinite-dimensional Lyapunov-based control for a flexible Cartesian robot with a piezoelectric patch actuator attachment. The robot was modeled as a flexible cantilever beam with a translational base support and a tip mass. The controller was designed to exponentially suppress the vibration of the beam and regulate the base motion. Coron et al. [24] presented a strict Lyapunov function for hyperbolic systems of conservation laws. The time derivative of this Lyapunov function can be made strictly negative definite by an appropriate choice of the boundary conditions. The method was illustrated by a hydraulic application. Cheng et al. [25] proposed sliding-mode boundary control of a one-dimensional unstable heat conduction system modeled by parabolic PDE systems with parameter variations and boundary uncertainties. An infinite-dimensional sliding manifold was constructed via Lyapunov's direct method. Simulation studies were conducted to verify the effectiveness of the sliding mode control law. In [26], Shang and Xu proposed a new control strategy for a one-dimensional cantilever Euler-Bernoulli beam with an input delay. The control system is either exponentially or asymptotically stable, depending on the time delay. In [27], Guo and Jin presented an active disturbance rejection and sliding mode control approach for a stabilization problem of Euler-Bernoulli beams with boundary input disturbance. The controller design is based on a PDE model. In [28], Luemchamloey and Kuntanapreeda presented an experimental study of active vibration control of flexible beams. The flexible beam was modeled by PDE. The controller was designed based on the infinite-dimensional Lyapunov method. He et al. [29] considered vibration control of a flexible string system. With Lyapunov's direct method, adaptive boundary control was developed to suppress the string's vibration and the adaptive law was designed to compensate for the system parametric uncertainties. Numerical simulations were carried out to verify the effectiveness of the controller.

In addition, high-order sliding-mode differentiation [30, 31] has been attracting interest. It is an alternative differentiation that features robust exact differentiation with finite-time convergence. It has been successfully used in control laws, replacing the use of derivative measurements [32, 33].

This paper presents an adaptive feedback control law to suppress vibration of Euler-Bernoulli beams with a collocated piezoelectric actuator/sensor pair. The actuator and sensor are lead zirconate titanate (PZT). The filtered signal from the sensor is used to provide the feedback signal. The governing equation of the beams is a PDE. Thus, it has an infinite number of vibration modes. The controller is designed based on an infinite-dimensional Lyapunov method, which does not involve any approximated finite-dimensional models. Thus, the stability of the control system including the filter dynamic is guaranteed for all vibration modes. The high-order differentiation is used to estimate the derivative of the sensor signal and then used in the control law. The rest of the paper is organized as follows. Section 2 provides some preliminaries. Section 3 describes the flexible beam that is used as an experimental test bench. Section 4 presents a finite element model of the experimental beam. The proposed controller design is given in Section 5. Simulation and experimental results are presented in Section 6. The last section concludes the paper.

2. Preliminaries

2.1. System Modeling. Consider a flexible cantilever beam with piezoelectric actuator and sensor patches. The patches are bonded on the top and bottom surfaces of the beam as shown in Figure 1. A governing equation of the beam can be derived based on an Euler-Bernoulli beam equation and Hamilton's principle [19] as

$$\ddot{w}(x,t) = \frac{1}{\rho(x)}\left[M_{po}u(t)S''(x) - \frac{\partial^2\left(EI(x)w''(x,t)\right)}{\partial x^2} - B\dot{w}(x,t) - C\dot{w}'(x,t)\right], \tag{1}$$

with the boundary conditions

$$w(0,t) = \dot{w}(0,t) = w'(0,t) = 0, \quad w''(L,t) = w'''(L,t) = 0, \tag{2}$$

where the dot and prime notations represent derivatives with respect to time and the variable x, respectively, $w(x,t)$ is the transverse displacement of the beam, $u(t)$ is the input voltage applied to the actuator, L is the length of the beam, $\rho(x) = b_b\rho_b t_b + b_p\rho_p t_p S(x)$, ρ_b, ρ_p are the densities of the beam and the piezoelectric patch actuator, respectively, b_b, b_p are the widths of the beam and the actuator, t_b, t_p are the thicknesses of the beam and the actuator, $S(x) = H(x - l_1) - H(x - l_2)$,

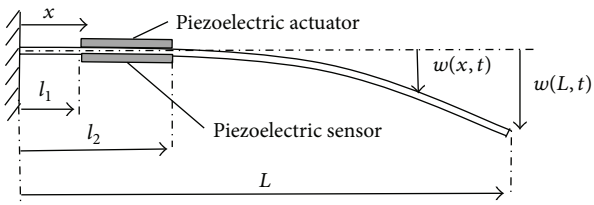

Figure 1: Beam with a piezoelectric actuator and a piezoelectric sensor.

$H(x)$ is the Heaviside function, l_1, l_2 are the distances from the clamped end to the leading edge and the tailing edge of the actuator, respectively, $M_{po} = -b_p E_p d_{31}(t_b + t_p)$ is the moment constant of the actuator, $EI(x) = EI_b + EI_p S(x)$ is the bending stiffness, $EI_p = 2b_p E_p t_p(t_b^2/4 + t_b t_p/2 + t_p^3/3)$ $EI_b = (E_b b_b t_b^3)/12$, E_b, E_p are the Young's moduli of the beam and the actuator, and B, C are the viscous and structural damping coefficients, respectively.

The equation relating the applied voltage u and the axial strain ε_{xx} produced by the piezoelectric patch actuator is written as [8, 11]:

$$\varepsilon_{xx} = d_{31}\frac{u}{t_p}, \tag{3}$$

where d_{31} and t_p are the dielectric constant and the thickness of the actuator, respectively. The normal stress σ_{xx} and the bending moment M_a on the beam produced by the actuator are

$$\sigma_{xx} = E_p d_{31}\frac{u}{t_p}, \tag{4}$$

$$M_a = \int_{t_b/2}^{t_b/2+t_p} \sigma_{xx} z\, dA = E_p d_{31} b_p \overline{z} u, \tag{5}$$

where E_p is Young's modulus of the actuator, b_p is the width of the actuator, $\overline{z} = (t_b + t_p)/2$, and t_b, t_p are the thicknesses of the beam and the actuator.

By considering the piezoelectric patch sensor as a parallel plate capacitor, the voltage $v_s(t)$ across the two layers produced by the sensor is given as [23]:

$$v_s(t) = \psi\left(w'(l_2, t) - w'(l_1, t)\right), \tag{6}$$

where $\psi = b_{p,s} E_{p,s} d_{31,s}(t_b + t_{p,s})/2C_{p,s}$ is the piezoelectric constant, $b_{p,s}$ is the width of the sensor, $E_{p,s}$ is Young's modulus of the sensor, $d_{31,s}$ is the dielectric constant of the sensor, $t_{p,s}$ is the thickness of the sensor, and $C_{p,s}$ is the piezoelectric capacitance.

2.2. Finite Element Equation. Consider a finite element (FE) model of a cantilever beam shown in Figure 2. It is assumed that the beam is divided into n elements. Each element has two nodes and each node has two degrees of freedom: transverse direction (w_1, w_2) and slope (w_1', w_2').

The transverse displacement at any x position on the element can be expressed as [8, 30]:

$$[w(x)] = [\Phi]^T [q], \tag{7}$$

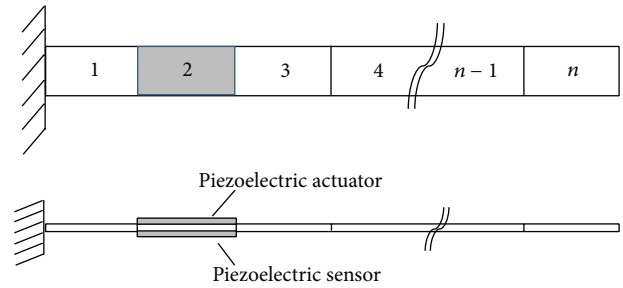

Figure 2: Finite element model.

where $[q]^T = [w_1 \;\; w_1' \;\; w_2 \;\; w_2']$ is the nodal displacement vector and $[\Phi] = [\phi_1 \;\; \phi_2 \;\; \phi_3 \;\; \phi_4]$ is the mode-shape vector function. By using the Lagrangian method, the differential equation of motion to be solved can be expressed as [34, 35]:

$$[M]\{\ddot{q}\} + [C]\{\dot{q}\} + [K]\{q\} = \{F\}, \tag{8}$$

where $[M] = \rho A \int_0^L \Phi^T \Phi\, dx$ is the mass matrix, $[K] = EI \int_0^L \Phi''^T \Phi'' dx$ is the stiffness matrix, $[C]$ is the damping matrix, and $\{F\}$ is the force matrix. For Rayleigh proportional damping, $C = \alpha M + \beta K$, where α, β are the damping constants. The force matrix $\{F\}$ for the element without the piezoelectric actuator is $\{F\} = [0 \;\; 0 \;\; 0 \;\; 0]^T$ and is, for the element bonded with the actuator, patch $\{F\} = [0 \;\; E_p d_{31} b_p \overline{z} \;\; 0 \;\; -E_p d_{31} b_p \overline{z}]^T u$, which is directly derived from (5). Note that the piezoelectric sensor is not included in the FE model since the bonded sensor in the experimental system is very thin and light compared to those of the beam and the actuator.

2.3. High-Order Sliding-Mode Differentiation. In this subsection, a high-order sliding-mode differentiation method is shortly described. To explain the method, let $f(t)$ be a function from which we want to determine its derivative. Consider the following auxiliary system:

$$\dot{z} = \eta. \tag{9}$$

The main idea is to find η to keep $z - f(t) = 0$, resulting in $\eta = \dot{f}(t)$. Based on a second-order sliding-mode algorithm, one obtains [30]

$$\begin{aligned} \eta &= \eta_1 - \mu_1 \left|z - f(t)\right|^{1/2} \operatorname{sign}\left(z - f(t)\right), \\ \dot{\eta}_1 &= -\mu_2 \operatorname{sign}\left(z - f(t)\right), \end{aligned} \tag{10}$$

where $\mu_1, \mu_2 > 0$ and sign (x) is a signum function. A general form of nth-order differentiators can be written as

$$\begin{aligned} \dot{\eta}_0 = \kappa_0, \quad \kappa_0 &= -\mu_0 \Gamma^{1/(n+1)} \left|\eta_0 - f(t)\right|^{n/(n+1)} \\ &\times \operatorname{sign}\left(\eta_0 - f(t)\right) + \eta_1, \end{aligned}$$

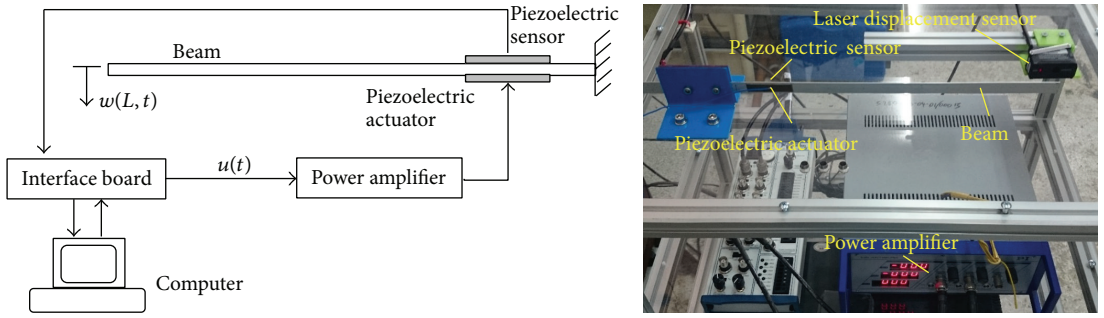

(a) (b)

Figure 3: Experimental system: (a) schematic and (b) photograph.

$$\dot{\eta}_1 = \kappa_1, \quad \kappa_1 = -\mu_1 \Gamma^{1/n} \left|\eta_1 - \kappa_0\right|^{(n-1)/n} \operatorname{sign}\left(\eta_0 - \kappa_0\right) + \eta_2,$$

$$\vdots$$

$$\dot{\eta}_{n-1} = \kappa_{n-1}, \quad \kappa_{n-1} = -\mu_{n-1} \Gamma^{1/2} \left|\eta_{n-1} - \kappa_{n-2}\right|^{1/2} \times \operatorname{sign}\left(\eta_{n-1} - \kappa_{n-2}\right) + \eta_n,$$

$$\dot{\eta}_n = -\mu_n \Gamma \operatorname{sign}\left(\eta_n - \kappa_{n-1}\right), \tag{11}$$

where η_n is an approximated value of the nth derivative of the function $f(t)$, $\Gamma > 0$ is a Lipschitz constant of the function $f(t)$, and μ_i $(i = 0, 1, \ldots, n)$ are constant parameters. The reader is referred to Levant [30, 31] for full details of the method. In this paper, this method will be used for estimating the first derivative of the signal from the piezoelectric sensor.

3. Experimental System

A schematic and a photograph of the experimental system used in this paper are shown in Figure 3. The system consists of a flexible cantilever beam, a piezoelectric patch actuator, a piezoelectric patch sensor, a high-voltage power amplifier, a 16-bit ADC/DAC interface board, and a PC. The beam is made of aluminum. The dimensions and properties of the beam are summarized in Table 1. The piezoelectric actuator and sensor are lead zirconate titanate (PZT). They are bonded on the beam at the distance $x = 15$ mm from the clamped point. The dimensions and properties of the actuator and sensor are summarized in Table 2. The sensor measures the axial strain of the beam. The system is also equipped with a laser displacement sensor for measuring the beam's tip deflection; however, the displacement sensor is not used in the control loop. The signals from the sensors are fed back to the PC through the interface board. The control signal from the computer is converted to an analogue signal by the interface board and is transmitted through the high-voltage power amplifier to the actuator to close the control loop. The gain of the amplifier is 150. Figure 4 displays the pulse response and the frequency response functions of the beam where the signal from the piezoelectric sensor is considered as the output. The frequency response shows that the first two natural frequencies of the beam are 39.28 rad/s and 224.7 rad/s.

Table 1: Beam's dimensions and properties.

Dimensions/properties	Symbol	Value	Unit
Young's modulus	E_b	70	GPa
Density	ρ_b	2700	kg/m^3
Poisson ratio	ν	0.35	—
Length	L	340	mm
Width	b_b	15	mm
Thickness	t_b	0.8	mm

Table 2: Piezoelectric material's dimensions and properties.

Dimensions/properties	Symbol	Value	Unit
Actuator			
Young's modulus	E_p	66.67	GPa
Density	ρ_p	7800	kg/m^3
Length	l_p	45	mm
Width	b_p	15	mm
Thickness	t_p	0.5	mm
Strain coefficient	d_{31}	$-171e^{-12}$	m/V
Piezoelectric position	l_1	15	mm
	l_2	60	mm
Sensor			
Young's modulus	$E_{p,s}$	2.5	GPa
Length	$l_{p,s}$	45	mm
Width	$b_{p,s}$	15	mm
Thickness	$t_{p,s}$	0.5	mm
Piezoelectric capacitance	$C_{p,s}$	$379e^{-12}$	Farad
Strain coefficient	$d_{31,s}$	$23e^{-12}$	m/V

4. Finite Element Model

A finite element (FE) model of the experimental beam was developed to be used in the control design process. For

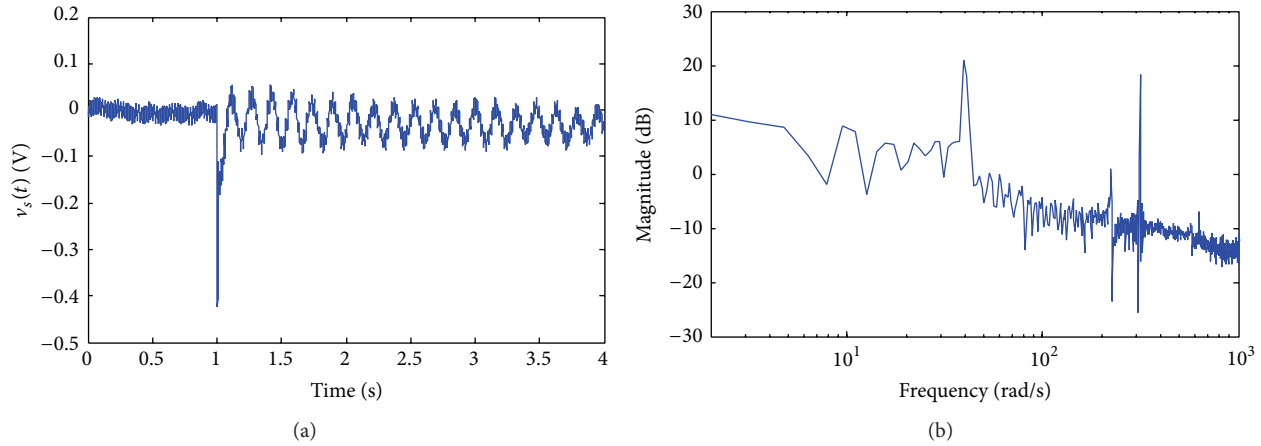

Figure 4: Experimental system's responses: (a) pulse response and (b) frequency response function.

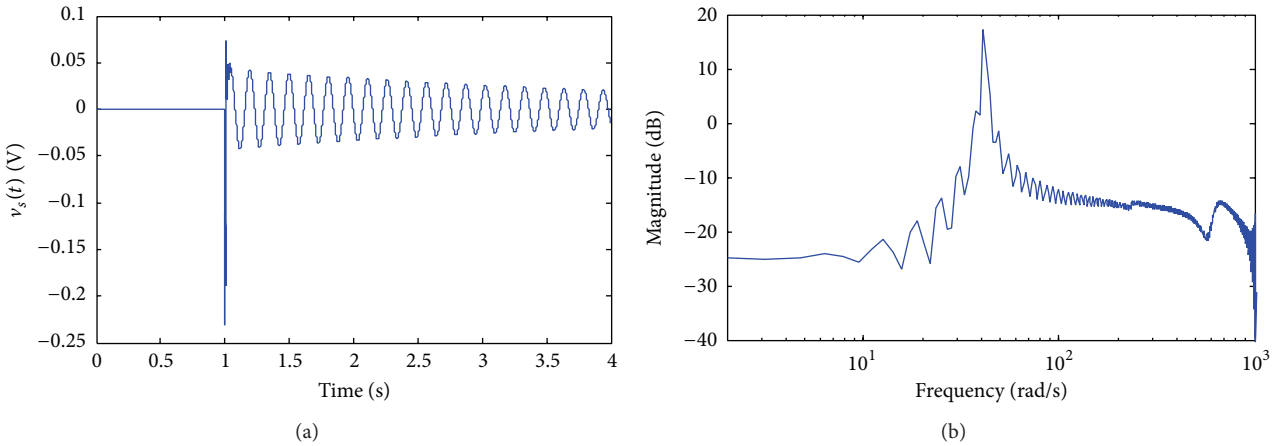

Figure 5: System's responses based on FE model: (a) pulse response and (b) frequency response function.

simplicity, $n = 11$ was chosen. The pulse response and the frequency response functions obtained from the developed FE model are shown in Figure 5. The responses agree with those of the experimental system.

5. Controller Design

The proposed control design is given in this section. The control objective is to suppress the vibration of the beam by using only the signal from the piezoelectric sensor. The schematic for the control loop is shown in Figure 6.

Instead of directly using v_s and $\dot{v}_s$ for feedback, let v_s and $\dot{v}_s$ pass through a low-pass filter to obtain a new feedback signal $y(t)$ as follows:

$$\dot{y}(t) = \frac{1}{\tau}\left(a_1 v_s(t) + a_2 \dot{v}_s(t) - y(t)\right), \tag{12}$$

where $\tau > 0$ is the time constant of the filter and $a_1, a_2 \geq 0$ $(a_1 + a_2 \neq 0)$ are weighting parameters. Note that including a low-pass filter in the control loop is usually done in practice

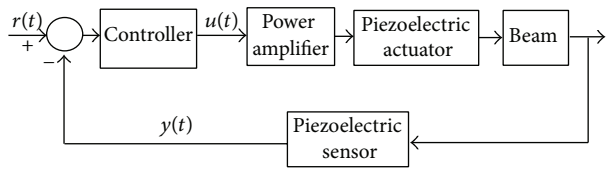

Figure 6: Controlled system.

to attenuate the effect of noise in the feedback signal. In the following, the dynamic of the filter is also included in the controller design.

Define a Lyapunov function candidate as

$$V_1 = \frac{1}{2M_{po}}\int_0^L \rho(x)\,\dot{w}^2(x,t)\,dx + \frac{1}{2M_{po}}\int_0^L EI(x)\,w''^2(x,t)\,dx + \frac{\lambda}{2}y^2, \tag{13}$$

where λ is considered as a controller parameter. By taking the time derivative of (13) and substituting (1), (2), (6), and (12) into the derivative result, it yields

$$\begin{aligned}\dot{V}_1 &= -\frac{B}{M_{po}}\int_0^L \dot{w}^2(x,t)\,dx \\ &\quad -\frac{C}{2M_{po}}\dot{w}^2(L,t)+u(t)\left(\dot{w}'(l_2,t)-\dot{w}'(l_1,t)\right) \\ &\quad +\frac{\lambda y}{\tau}\left(a_1\psi\left(w'(l_2,t)-w'(l_1,t)\right)\right. \\ &\qquad \left.+a_2\psi\left(\dot{w}'(l_2,t)-\dot{w}'(l_1,t)\right)-y\right) \\ &= -\frac{B}{M_{po}}\int_0^L \dot{w}^2(x,t)\,dx \\ &\quad -\frac{C}{2M_{po}}\dot{w}^2(L,t)-\frac{\lambda y^2}{\tau}+u(t)\left(\dot{w}'(l_2,t)-\dot{w}'(l_1,t)\right) \\ &\quad +\frac{\lambda y}{\tau}\left(a_1\psi\left(w'(l_2,t)-w'(l_1,t)\right)\right. \\ &\qquad \left.+a_2\psi\left(\dot{w}'(l_2,t)-\dot{w}'(l_1,t)\right)\right).\end{aligned} \tag{14}$$

By choosing the following control law:

$$u(t) = -\frac{\lambda a_2\psi y}{\tau}-\frac{\lambda a_1\psi y}{\tau}\frac{\left(w'(l_2,t)-w'(l_1,t)\right)}{\left(\dot{w}'(l_2,t)-\dot{w}'(l_1,t)\right)}, \tag{15}$$

it yields

$$\begin{aligned}\dot{V}_1 &= -\frac{B}{M_{po}}\int_0^L \dot{w}^2(x,t)\,dx-\frac{C}{2M_{po}}\dot{w}^2(L,t)-\frac{\lambda y^2}{\tau} \\ &\le -\frac{\lambda y^2}{\tau}\le 0.\end{aligned} \tag{16}$$

By Barbalat's lemma [36, 37], $y \to 0$ is achieved. Note that $w'(l_2,t) - w'(l_1,t)$ can be obtained directly from the piezoelectric sensor (6); that is, $v_s(t) = \psi(w'(l_2,t) - w'(l_1,t))$, and $\dot{w}'(l_2,t) - \dot{w}'(l_1,t)$ can be obtained from $\dot{v}_s(t)$. In our experiment, we used the high-order sliding-mode differentiation method described in Section 2.3 to determine $\dot{v}_s(t)$.

Note that control law (15) has a singularity at $\dot{w}'(l_2,t) - \dot{w}'(l_1,t) = 0$. Thus, implementations of the control law must empirically avoid this singularity. For simplicity, we chose $a_1 = 0$ and $a_2 = 1$ in the experiment to avoid the singularity.

Moreover, the parameter ψ is usually uncertain or even unknown. Thus, control law (15) with $a_1 = 0$ and $a_2 = 1$ is modified as

$$u = -\frac{\lambda k(t)\,y}{\tau}, \tag{17}$$

where $k(t)$ is an adaptive variable replacing ψ. Define $e(t) = k(t) - \psi$. Take

$$\begin{aligned}V &= V_1+\frac{1}{2}e^2 \\ &= \frac{1}{2M_{po}}\int_0^L \rho(x)\,\dot{w}^2(x,t)\,dx \\ &\quad +\frac{1}{2M_{po}}\int_0^L EI(x)\,w''^2(x,t)\,dx+\frac{\lambda}{2}y^2\end{aligned} \tag{18}$$

as a new Lyapunov function candidate. Taking its derivative with respect to time and substituting (17) into the result yields

$$\begin{aligned}\dot{V} &= -\frac{B}{M_{po}}\int_0^L \dot{w}^2(x,t)\,dx-\frac{C}{2M_{po}}\dot{w}^2(L,t) \\ &\quad +\left(-\frac{\lambda k(t)\,y}{\tau}\right)\left(\dot{w}'(l_2,t)-\dot{w}'(l_1,t)\right) \\ &\quad +\frac{\lambda y}{\tau}\left(\psi\left(\dot{w}'(l_2,t)-\dot{w}'(l_1,t)\right)-y\right) \\ &\quad +\left(k(t)-\psi\right)\dot{k}(t) \\ &= -\frac{B}{M_{po}}\int_0^L \dot{w}^2(x,t)\,dx-\frac{C}{2M_{po}}\dot{w}^2(L,t)-\frac{\lambda y^2}{\tau} \\ &\quad +\left(\dot{k}(t)-\frac{\lambda y\left(\dot{w}'(l_2,t)-\dot{w}'(l_1,t)\right)}{\tau}\right)\left(k(t)-\psi\right).\end{aligned} \tag{19}$$

By choosing the following adaptive law:

$$\dot{k}(t) = \frac{\lambda y\left(\dot{w}'(l_2,t)-\dot{w}'(l_1,t)\right)}{\tau}, \tag{20}$$

it results in

$$\begin{aligned}\dot{V} &= -\frac{B}{M_{po}}\int_0^L \dot{w}^2(x,t)\,dx-\frac{C}{2M_{po}}\dot{w}^2(L,t)-\frac{\lambda y^2}{\tau} \\ &\le -\frac{\lambda y^2}{\tau}\le 0.\end{aligned} \tag{21}$$

Applying Barbalat's lemma [36, 37] results in $y \to 0$.

6. Results

6.1. Simulation Study. A simulation study was conducted using the FE model described in Section 2.2 to tune the control parameter λ. It was observed that the convergence rate of the controlled response increases with λ. Here, the control gain of $\lambda = 0.052$ was chosen. Simulation results

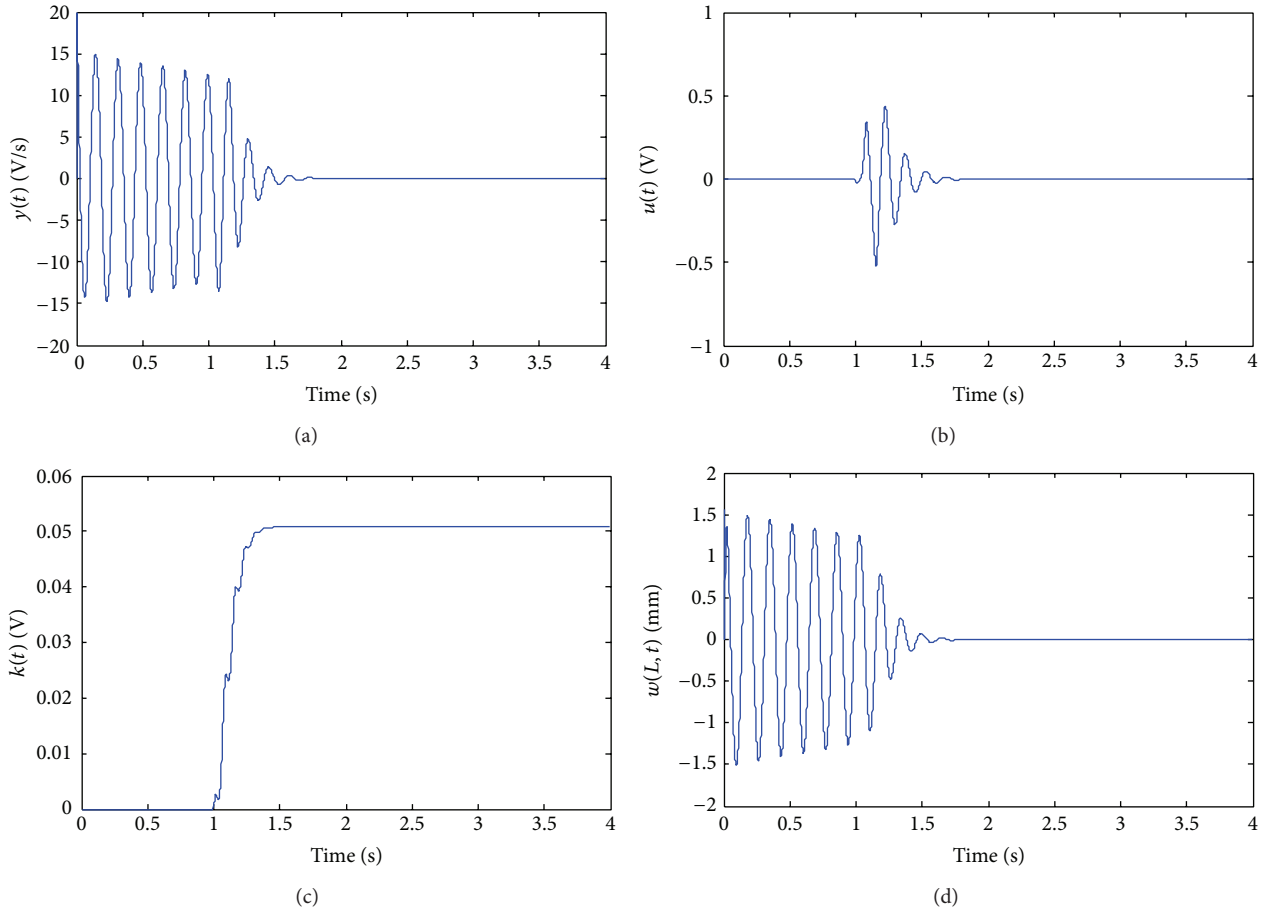

FIGURE 7: FEM simulation result (the controller was activated at $t = 1$ sec): (a) feedback signal, (b) control signal, (c) adaptive variable, and (d) tip deflection.

are shown in Figure 7. The controller was activated at $t = 1$ sec. The results show that the controller is able to suppress the vibration effectively. Note that $k(t)$ converged to a finite value.

6.2. Experimental Results. Controller (17) was implemented digitally on the PC with the sampling period of the control loop of 1 msec. The high-order sliding differentiation technique with $\Gamma = 700$, $\mu_0 = \mu_1 = 1$, was used. The experimental results are shown in Figure 8. The controller provides satisfactory responses similar to those obtained by the simulation. Note that the controller was activated at $t = 1$ sec.

Note that we set the initial conditions of the FEM simulation and experiment roughly the same for a comparison purpose. It was found that there are slight differences in the FEM simulation and experimental results. This is mainly due to the measurement noise and the mismatch in the initial conditions. The difference between the maximum control inputs is about 12.08%. The difference of the steady state adaptive gains is about 3.35%. In summary, both results are practically comparable.

7. Conclusions

In this paper we proposed an adaptive controller for vibration suppression of flexible structures. The structure under consideration is a cantilever beam with a collocated piezoelectric actuator and sensor pair. The governing equation of the beam is a partial differential equation. Since the beam is an infinite-dimensional system, we derived the control law using the infinite-dimensional Lyapunov method, which does not require any approximated finite-dimension model. Thus, the stability of the control system is guaranteed for all vibration modes. We also employed a high-order sliding mode differentiation technique to obtain the derivative of the sensor's signal for being used in the control law. The technique features robust exact differentiation with finite-time convergence. Effectiveness of the controller is illustrated both in finite-element model and experiment, with results that show good agreement.

Conflict of Interests

The authors declare that there is no conflict of interests regarding the publication of this paper.

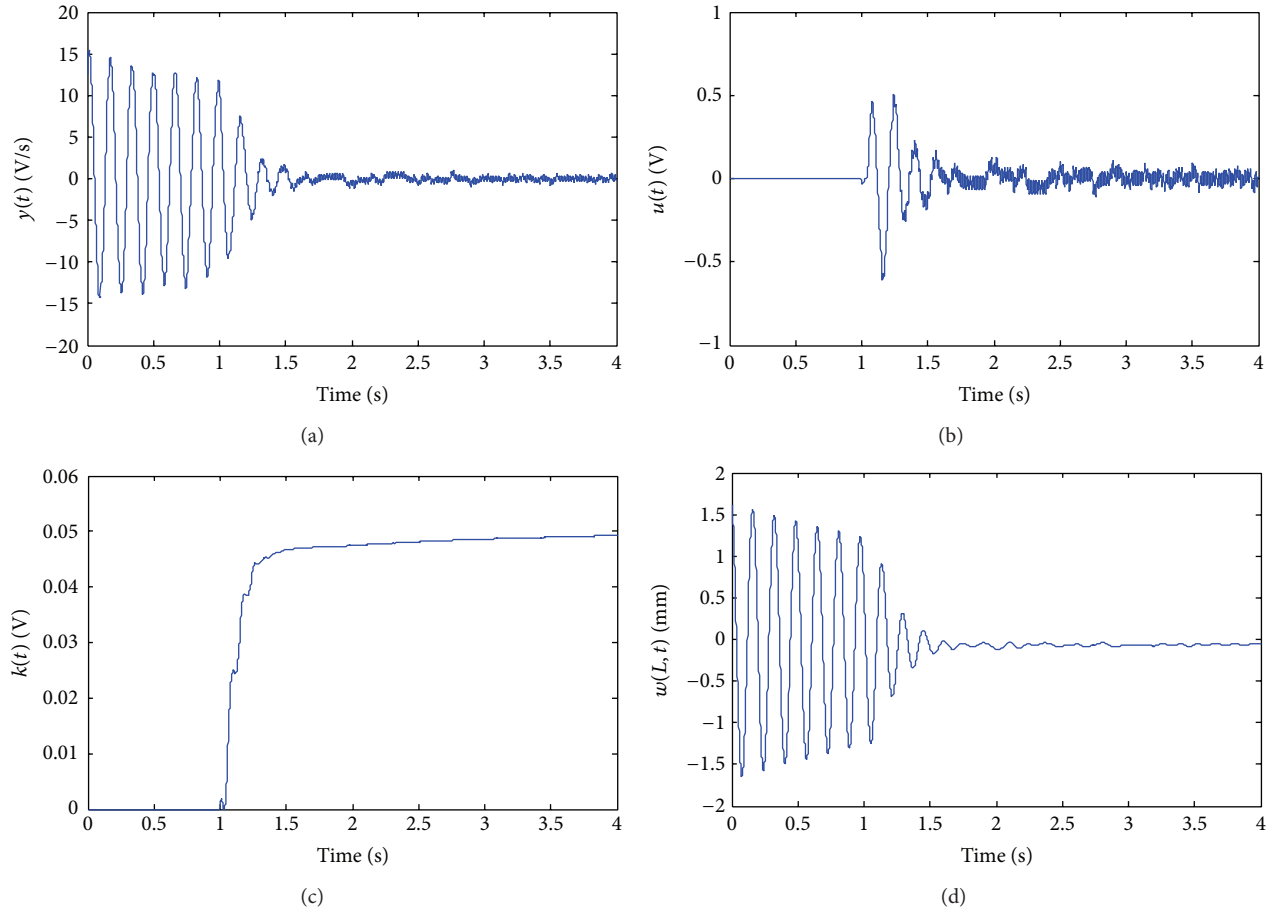

FIGURE 8: Experimental result (the controller was activated at $t = 1$ sec): (a) feedback signal, (b) control signal, (c) adaptive variable, and (d) tip deflection.

Acknowledgments

This work was supported by the Royal Golden Jubilee Ph.D. program of the Thailand Research Fund. The authors also would like to thank anonymous referees for their valuable comments.

References

[1] Z. Mohamed, J. M. Martins, M. O. Tokhi, J. Sá da Costa, and M. A. Botto, "Vibration control of a very flexible manipulator system," *Control Engineering Practice*, vol. 13, no. 3, pp. 267–277, 2005.

[2] M. Azadi, S. A. Fazelzadeh, M. Eghtesad, and E. Azadi, "Vibration suppression and adaptive-robust control of a smart flexible satellite with three axes maneuvering," *Acta Astronautica*, vol. 69, no. 5-6, pp. 307–322, 2011.

[3] T. P. Sales, D. A. Rade, and L. C. G. De Souza, "Passive vibration control of flexible spacecraft using shunted piezoelectric transducers," *Aerospace Science and Technology*, vol. 29, no. 1, pp. 403–412, 2013.

[4] C. C. Fuller, *Active Control of Vibration*, Academic Press, 1996.

[5] A. Preumont, *Vibration Control of Active Structures*, Kluwer Academic, 1997.

[6] A. M. Aly, "Vibration control of buildings using magnetorheological damper: a new control algorithm," *Journal of Engineering*, vol. 2013, Article ID 596078, 10 pages, 2013.

[7] A. Moutsopoulou, G. E. Stavroulakis, and A. Pouliezos, "Innovation in active vibration control strategy of intelligent structures," *Journal of Applied Mathematics*, vol. 2014, Article ID 430731, 14 pages, 2014.

[8] B. Bandyopadhyay, T. C. Manjunath, and M. Umapathy, *Modeling, Control and Implementation of Smart Structures: A FEM-State Space Approach*, Springer, Berlin, Germany, 2007.

[9] A. R. Tavakolpour, M. Mailah, I. Z. Mat Darus, and O. Tokhi, "Self-learning active vibration control of a flexible plate structure with piezoelectric actuator," *Simulation Modelling Practice and Theory*, vol. 18, no. 5, pp. 516–532, 2010.

[10] H. Wang, X.-H. Shen, L.-X. Zhang, and X.-J. Zhu, "Active vibration suppression of flexible structure using a LMI-based control patch," *Journal of Vibration and Control*, vol. 18, no. 9, pp. 1375–1379, 2012.

[11] Z. Qiu, X. Zhang, and C. Ye, "Vibration suppression of a flexible piezoelectric beam using BP neural network controller," *Acta Mechanica Solida Sinica*, vol. 25, no. 4, pp. 417–428, 2012.

[12] T. Sangpet, S. Kuntanapreeda, and R. Schmidt, "Improving delay-margin of noncollocated vibration control of piezo-actuated flexible beams via a fractional-order controller," *Shock and Vibration*, vol. 2014, Article ID 809173, 8 pages, 2014.

[13] F. An, W. Chen, and M. Shao, "Dynamic behavior of time-delayed acceleration feedback controller for active vibration control of flexible structures," *Journal of Sound and Vibration*, vol. 333, no. 20, pp. 4789–4809, 2014.

[14] G. Takács, T. Polóni, and B. Rohal'-Ilkiv, "Adaptive model predictive vibration control of a cantilever beam with real-time parameter estimation," *Shock and Vibration*, vol. 2014, Article ID 741765, 15 pages, 2014.

[15] T. Sangpet, S. Kuntanapreeda, and R. Schmidt, "Hysteretic nonlinearity observer design based on Kalman filter for piezo-actuated flexible beams," *International Journal of Automation and Computing*, vol. 11, no. 6, pp. 627–634, 2014.

[16] X. Dong, Z. Peng, W. Zhang, H. Hua, and G. Meng, "Research on spillover effects for vibration control of piezoelectric smart structures by ANSYS," *Mathematical Problems in Engineering*, vol. 2014, Article ID 870940, 8 pages, 2014.

[17] A. Montazeri, J. Poshtan, and A. Yousefi-Koma, "Design and analysis of robust minimax LQG controller for an experimental beam considering spill-over effect," *IEEE Transactions on Control Systems Technology*, vol. 19, no. 5, pp. 1251–1259, 2011.

[18] R. Padhi and S. F. Ali, "An account of chronological developments in control of distributed parameter systems," *Annual Reviews in Control*, vol. 33, no. 1, pp. 59–68, 2009.

[19] S. Zhao, H. Lin, and Z. Xue, "Switching control of closed quantum systems via the Lyapunov method," *Automatica*, vol. 48, no. 8, pp. 1833–1838, 2012.

[20] S. Kuntanapreeda and P. M. Marusak, "Nonlinear extended output feedback control for CSTRs with van de Vusse reaction," *Computers & Chemical Engineering*, vol. 41, pp. 10–23, 2012.

[21] B. Zhang, K. Liu, and J. Xiang, "A stabilized optimal nonlinear feedback control for satellite attitude tracking," *Aerospace Science and Technology*, vol. 27, no. 1, pp. 17–24, 2013.

[22] A. Yang, W. Naeem, G. W. Irwin, and K. Li, "Stability analysis and implementation of a decentralized formation control strategy for unmanned vehicles," *IEEE Transactions on Control Systems Technology*, vol. 22, no. 2, pp. 706–720, 2014.

[23] M. Dadfarnia, N. Jalili, B. Xian, and D. M. Dawson, "A lyapunov-based piezoelectric controller for flexible cartesian robot manipulators," *Journal of Dynamic Systems, Measurement and Control*, vol. 126, no. 2, pp. 347–358, 2004.

[24] J.-M. Coron, B. d'Andréa-Novel, and G. Bastin, "A strict Lyapunov function for boundary control of hyperbolic systems of conservation laws," *IEEE Transactions on Automatic Control*, vol. 52, no. 1, pp. 2–11, 2007.

[25] M.-B. Cheng, V. Radisavljevic, and W.-C. Su, "Sliding mode boundary control of a parabolic PDE system with parameter variations and boundary uncertainties," *Automatica*, vol. 47, no. 2, pp. 381–387, 2011.

[26] Y. F. Shang and G. Q. Xu, "Stabilization of an Euler-Bernoulli beam with input delay in the boundary control," *Systems and Control Letters*, vol. 61, no. 11, pp. 1069–1078, 2012.

[27] B.-Z. Guo and F.-F. Jin, "The active disturbance rejection and sliding mode control approach to the stabilization of the Euler-Bernoulli beam equation with boundary input disturbance," *Automatica*, vol. 49, no. 9, pp. 2911–2918, 2013.

[28] A. Luemchamloey and S. Kuntanapreeda, "Active vibration control of flexible beam based on infinite-dimensional lyapunov stability theory: an experimental study," *Journal of Control, Automation and Electrical Systems*, vol. 25, no. 6, pp. 649–656, 2014.

[29] W. He, S. Zhang, and S. S. Ge, "Adaptive boundary control of a nonlinear flexible string system," *IEEE Transactions on Control Systems Technology*, vol. 22, no. 3, pp. 1088–1093, 2014.

[30] A. Levant, "Robust exact differentiation via sliding mode technique," *Automatica*, vol. 34, no. 3, pp. 379–384, 1998.

[31] A. Levant, "Higher-order sliding modes, differentiation and output-feedback control," *International Journal of Control*, vol. 76, no. 9-10, pp. 924–941, 2003.

[32] X. Wang and B. Shirinzadeh, "High-order nonlinear differentiator and application to aircraft control," *Mechanical Systems and Signal Processing*, vol. 46, no. 2, pp. 227–252, 2014.

[33] I. Salgado, I. Chairez, O. Camacho, and C. Yañez, "Super-twisting sliding mode differentiation for improving PD controllers performance of second order system," *ISA Transactions*, vol. 53, no. 4, pp. 1096–1106, 2014.

[34] S. Y. Wang, "A finite element model for the static and dynamic analysis of a piezoelectric bimorph," *International Journal of Solids and Structures*, vol. 41, no. 15, pp. 4075–4096, 2004.

[35] D. L. Logan, *A First Course in the Finite Element Method*, Wadsworth Group, 2002.

[36] J. E. Slotine, *Applied Nonlinear Control*, Prentice-Hall, 1991.

[37] H. K. Khalil, *Nonlinear Systems*, Prentice-Hall, 1996.